

Removal of Organic Films From Rotating Disks Using Aqueous Solutions of Nonionic Surfactants: Effect of Surfactant Molecular Structure

Jeffrey A. Kabin, Stephanie L. Tolstedt, A. Eduardo Sáez, Christine S. Grant,¹ and Ruben G. Carbonell

Department of Chemical Engineering, North Carolina State University, Box 7905, Raleigh, North Carolina 27695-7905

Received December 19, 1997; accepted May 28, 1998

In prior work, we examined the removal of abietic acid films from rotating fiberglass laminate disks by aqueous solutions of a nonionic surfactant. A three-stage cleaning mechanism was found, consisting successively of solubilization, shear-driven cleaning, and roll-up. We extend this work by exploring the influence of the surfactant molecular structure on the kinetics of the cleaning process. Five different poly(ethylene glycol) alkyl ether surfactants (C_xE_y) were used. Both the alkyl (*x*) and ethoxy (*y*) chain lengths were varied. Not all of the surfactants exhibited a three-stage cleaning mechanism. It was found that for surfactants with relatively high solubilization rates, the shear-driven cleaning stage did not occur. The selection of the most efficient surfactant depends on whether the surfactant concentration is below or above its critical micelle concentration (CMC). At submicellar concentrations, faster cleaning is obtained by surfactants that can induce shear-driven removal. At concentrations above the CMC, it is found that surfactant efficiency for a fixed alkyl or ethoxy chain length increases as the surfactant becomes more hydrophilic. This is attributed in part to the lower viscosity that the film achieves with the more hydrophilic surfactants due to their partitioning into the film, as well as their ability to carry water into the film. © 1998

Academic Press

Key Words: cleaning; abietic acid; solubilization; nonionic surfactant; hydrophile to lipophile balance.

INTRODUCTION

The removal of organic contaminants from solid surfaces is a topic of wide commercial and industrial importance. Traditionally, research in detergency has been associated with the removal of liquids and particulates from textile fabrics. Previous research on detergency has concentrated on the effects of interfacial phenomena on cleaning (1, 2). For example, when a micellar aqueous surfactant solution is contacted with an organic contaminant, one of the possible cleaning mechanisms is the solubilization of the organic into surfactant micelles. This process can be controlled either by mass transfer of the micelles or by the kinetics of the micellization process that occurs

at the interface. The cleaning rate associated with this process is therefore controlled by interfacial mechanisms. Other studies have pointed out that in certain applications, the liquefaction of the organic contaminant caused by surfactant and water partitioning might lead to improved cleaning (3, 4, 5). In this case, cleaning behavior is not only controlled by interfacial phenomena, but also by changes in the rheological properties of the liquefied contaminant.

It is widely accepted in the literature that the cleaning of organic residues from surfaces by aqueous surfactant solutions proceeds by one of three different mechanisms, solubilization, emulsification, or roll-up (2, 6). Solubilization is the dissolution of the contaminant directly into the cleaning agent in the form of micellar aggregates. Emulsification is dominated by contaminant/detergent interactions in which an emulsion phase is formed at the aqueous/organic interface. The emulsion is then removed from the surface by hydrodynamic forces. Roll-up is dependent on the solvent/substrate interactions. For roll-up to occur, the substrate must be wetted by the cleaning solution. When this occurs, the contaminant forms drops on the substrate with a relatively large contact angle. The drops proceed to separate from the substrate and are transported to the liquid phase. According to Rosen (6), roll-up (or roll back) is the usual mechanism in the cleaning of liquid organic contaminants from surfaces.

The efficacy of the cleaning process is often determined by the “detergent ability” of the cleaning agent. According to Rosen (6), “Detergency, when applied to a surface-active agent, means the special property it has of enhancing the cleaning power of a liquid.” Cleaning power is generally envisioned in terms of minimizing contaminant remaining on the substrate in the cleaning process. Less consideration has been given to the rate at which the contaminant is removed. This study focuses on the rates of detergency and the physical aspects that control them.

Cleaning Mechanisms and Kinetics

The kinetics of solubilization of organic components into aqueous surfactant solutions has been studied in the past

¹ To whom correspondence should be addressed. E-mail: grant@eos.ncsu.edu. Fax: (919) 515-3465.

using the rotating disk system (7) and the captive drop-on-fiber technique (8). Prior work by our group on the removal of organic films from the surface of rotating disks by aqueous surfactant solutions has shown that the kinetics of the cleaning process is complex. Earlier work by our group was concerned with the removal of flux residues from printed circuit boards. Abietic acid is a primary component of flux and was chosen as the contaminant. For abietic acid films on a rotating disk, the cleaning mechanism in the presence of pentaethylene glycol dodecyl ether ($C_{12}E_5$) was found to change from solubilization to shear-driven removal to roll-up (9–11). We have also determined that the efficiency of a surfactant in terms of removal rates is linked with its ability to penetrate the organic contaminant.

In the rotating disk system, Beaudoin *et al.* (9) and Kabin *et al.* (11) observed that the cleaning process consisted of three successive stages. A typical cleaning curve is shown in Fig. 1. In this figure, N_A represents the total moles of abietic acid removed from the disk at a given time t . At early times, an approximately linear cleaning stage was found, in which abietic acid removal was relatively slow (stage 1). At a specific onset time, denoted by t_c , the cleaning rate increased, abruptly leading to stage 2, in which typically most of the abietic acid removal took place. Finally, the cleaning rate substantially decreased (stage 3) and complete removal of the organic film occurred asymptotically with time. The transition from stage 2 to stage 3 is more gradual than the rate increase observed at the beginning of the second stage.

The first stage of cleaning consists of a solubilization mechanism in which abietic acid is dissolved into the aqueous phase in micellar aggregates. The process includes the following steps (Fig. 2):

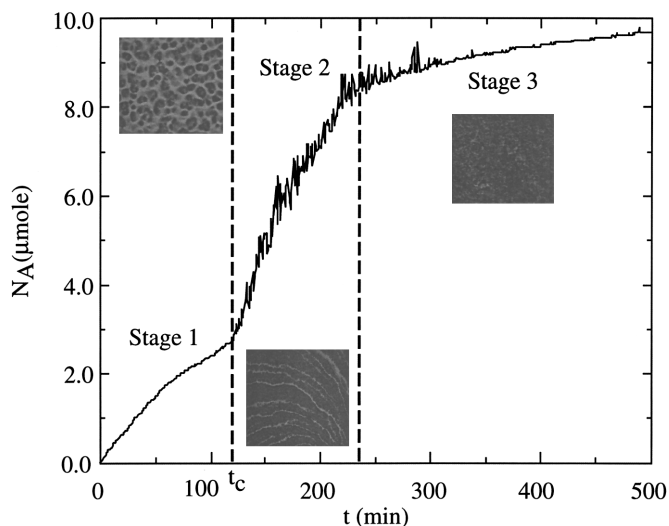
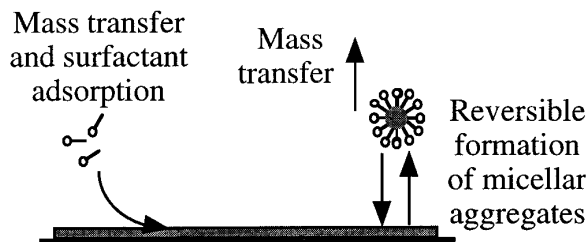
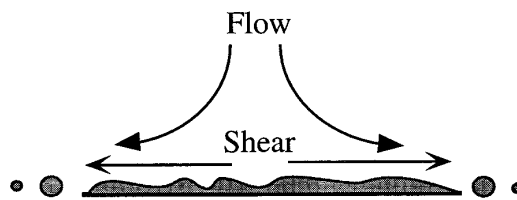


FIG. 1. Typical cleaning curve of an abietic acid film from a rotating disk. The submicellar cleaning solution is an aqueous solution of $C_{12}E_5$ with a concentration of $6.0 \times 10^{-5} M$. The rotational speed of the disk is 750 rpm. Photographs of the disk are shown during each stage of cleaning.

Stage 1: Solubilization



Stage 2: Shear removal



Stage 3: Roll up

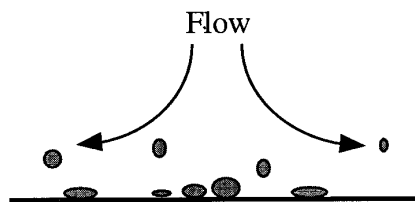


FIG. 2. Schematic of the three mechanisms of cleaning.

- Mass transfer of the surfactant from the bulk of the aqueous solution to the vicinity of the film surface.
- Adsorption of surfactant at the interface.
- Reversible formation of micellar aggregates containing abietic acid molecules that desorb from the interface into the aqueous phase.
- Mass transfer of micelles from the interface region to the bulk of the aqueous solution.

During the first cleaning stage the surfactant is transported into the organic phase, and water from the aqueous solution is being solubilized into the organic phase. As surfactant and water partition into the organic phase, the film begins to swell on the disk. Photographs of the film morphology have shown that during the first stage, the film breaks and forms a honeycomb structure (Fig. 1). The film then starts to move on the surface under the action of the shear stress exerted by the cleaning solution. This motion, which is enhanced by the reduced viscosity of the organic phase caused by surfactant and water absorption, leads to drop coalescence and the formation

of continuous films of organic phase (rivulets). The abietic acid flows along the rivulets towards the edge of the disk, from which drops detach into the cleaning solution (Fig. 1). We have shown that the spiral shape of these rivulets is determined by the direction of the shear stress exerted by the surfactant solution (11).

During the third stage, remnants of the rivulets are distributed in the form of isolated drops on the surface. Some of these drops maintain part of the original spiral shape of the rivulets. The removal of the remaining organic occurs by a roll-up mechanism (Fig. 2).

Kabin *et al.* (11) developed a mathematical model for the cleaning process during stage 1. In this model the controlling mechanisms are the net rate of removal of abietic acid micelles from the interface and their subsequent mass transfer into the bulk of the surfactant solution. The initial rate of removal is given by

$$\left. \frac{dN_A}{dt} \right|_{t=0} = k_1 = \frac{k_A A r_R}{k_A + k}, \quad [1]$$

where A is the disk surface area, k is the rate constant for the adsorption of abietic acid from micelles onto the interface, which is assumed to be linear in abietic acid concentration, k_A is the mass transfer coefficient of abietic acid micelles from the interface to the bulk of the aqueous phase, r_R is the specific rate of desorption of abietic acid from the film surface into the aqueous solution (moles of acid removed per unit of time and area). The initial cleaning rate in stage 1 (k_1) is therefore a function of surfactant concentration (mainly through r_R and k), and all the parameters that affect the mass transfer coefficient, which is given by

$$k_A = 0.6205 \nu_2^{-1/6} D_A^{2/3} \omega^{1/2}, \quad [2]$$

where ν_2 is the kinematic viscosity of the aqueous solution, D_A is the diffusion coefficient of the abietic acid micelles in the aqueous solution, and ω is the rotational speed. Experimental data at various rotational speeds and surfactant concentrations were in agreement with this model (11).

The second-stage cleaning process was modeled by analyzing the removal of organic phase induced by the shear stress acting on a rivulet. An expression was developed for the change in height of a rivulet of abietic acid on the disk with time. Based on this, the initial rate of abietic acid removal in the second stage was determined to be (11)

$$\left(\frac{dN_A}{dt} \right)_{t=t_c(\text{stage 2})} = k_2 = \frac{n_R W L \rho_1}{M} \frac{0.255 (\mu_2 \rho_2)^{1/2} \omega^{3/2}}{\mu_1} h_0^2, \quad [3]$$

where n_R is the number of rivulets on the disk, W is the width

of a rivulet, L is the length of a rivulet, ρ is the density (1, organic phase; 2, aqueous phase), μ is viscosity, and h_0 is the initial rivulet thickness. Experimentally, k_2 corresponds to the slope of the cleaning curve at the onset of stage 2 ($t = t_c$, Fig. 1). Beaudoin *et al.* (9) and Kabin *et al.* (11) have corroborated that there is a direct proportionality between k_2 and $\omega^{3/2}$, which is consistent with an induced shear represented by Eq. [3].

The previous analysis shows that film removal is influenced not only by the surfactant's ability to solubilize the contaminant but also by the partitioning of the surfactant into the organic phase, carrying water as it partitions (this affects μ_1 in Eq. [3]). Global cleaning rates might involve a complex interplay among the various cleaning stages. The complex nature of the cleaning process also makes it difficult to predict which specific surfactant would be best suited for a given contaminant/substrate combination. Previous works that have studied the influence of surfactant molecular structure on cleaning usually employ cleaning processes that occur by a single mechanism.

Effect of Surfactant Molecular Structure on Cleaning

Rosen (12) stated that surfactants consisting of a long and straight hydrophobic chain with a terminally located hydrophilic group were "good" detergents. According to this study, detergency becomes significant at or near the surfactant's critical micelle concentration, and increases with increasing hydrophobic chain length. For poly(ethylene glycol) alkyl ether surfactants, Rosen (12, 13) showed that an increase in the alkyl chain length resulted in a larger depression of surface tension of an aqueous solution. From this fact, he concluded that the longer the alkyl chain, the more effective the surfactant as a detergent. This theory was later corroborated by experimental studies performed by Ueno *et al.* (14).

The use of surface tension reduction as an indication of the detergent ability of a surfactant is consistent with the mechanisms of solubilization and roll-up. Lower surface tensions usually indicate lower CMCs and thus a larger potential for micellar solubilization (4). On the other hand, lower surface tensions (or, more rigorously, lower contaminant-aqueous solution interfacial tensions) might lead to larger contact angles of the organic phase on a solid substrate and thus to an improvement in roll-up.

In direct measurements involving cleaning processes, Chiu *et al.* (15), varied the ethoxy chain length for $C_{12}E_y$ surfactants from $y = 4$ to $y = 8$. They found that as y decreased, solubilization rates of nonpolar hydrocarbons increased. For C_xE_y surfactants, Harris *et al.* (16) observed that aqueous solutions started to remove contaminants from hard surfaces at or near the surfactant CMC and reached maximum detergency at concentrations well above the CMC. As a result they concluded that the nonionic surfactant CMC was a crucial parameter in comparing surfactant performance.

Diallo *et al.* (17) studied the effect of the surfactant hydro-

phile-lipophile balance number (HLB) on liquid hydrocarbon solubility. The HLB is defined by

$$\text{HLB} = 20 \frac{M_H}{M_H + M_L}, \quad [4]$$

where M_H and M_L are the formula masses of the surfactant molecule hydrophilic and hydrophobic portions, respectively. Diallo *et al.* used micellar solutions of $C_{12}E_y$, with $y = 6$ to 31 to solubilize various hydrocarbons. Their general conclusion was that the solubilization capacity of the surfactant solution decreased as HLB increased. However, for benzene and chlorobenzenes, the solubilization capacity increased with HLB, reached a maximum, and then decreased. Diallo *et al.* interpreted these results in terms of possible interactions between the surfactant ethylene oxide groups and the aromatic rings within the micelle. It is interesting to notice that, depending on the nature of the contaminant, solubilization trends with HLB might vary (17).

Surfactant molecular structure also plays a role when the cleaning process is affected by surfactant and water partitioning into the contaminant. Cox and Matson (3) studied the penetration of polyoxyethylenated nonionic surfactants into solid lard, concluding that penetration could be a primary controlling contaminant removal mechanism in hard surface cleaning. They concluded that the ability of a nonionic surfactant to penetrate into a contaminant could be strongly related to the surfactant carbon chain length: surfactants with smaller hydrophobic portions could penetrate into the contaminant at a faster rate, causing it to liquefy. In a related study, Cox (4) found that the C_8E_y surfactants' rate of penetration into three different contaminants was significantly higher than that of the $C_{12}E_y$ surfactants. This agreed with Cox and Matson's (3) previous findings. Based on these experiments, Cox recommended that in hard surface cleaning applications involving mechanical action, a nonionic surfactant which maximizes contaminant penetration should be used. This would require

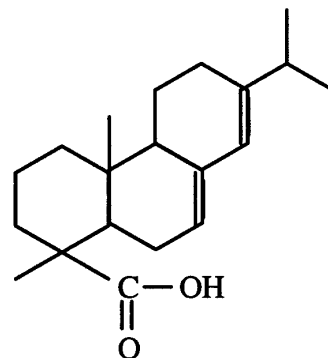


FIG. 4. Molecular structure of abietic acid.

minimizing both the carbon chain length and the surfactant water solubility.

The results discussed above show that selection of the best surfactant for a specific application depends on the nature of the contaminant and the mechanism that controls the cleaning process. In this work we will establish criteria for selecting the most appropriate surfactant for the removal of abietic acid films, an application that involves a complex cleaning mechanism.

MATERIALS AND METHODS

A detailed description of the experimental apparatus and measuring techniques is given elsewhere (9, 11). Here we will present only a summary of equipment and procedures. A schematic diagram of the experimental setup is shown in Fig. 3.

The FR-4 laminate disks (2.1 cm in diameter) were spin coated with one application of a 42% by weight solution of abietic acid (AA) in isopropyl alcohol. The molecular structure of abietic acid is shown in Fig. 4. After the coating process, the disks were placed in a dessicator at room temperature for 24 h and then stored in a refrigerator. It was determined that the film of abietic acid solution on the disk had an initial thickness of approximately 10 μm (9), and it was a viscous liquid that consisted of a solution of approximately 75% by weight abietic acid in isopropyl alcohol. The change in abietic acid content is due to alcohol evaporation during spin coating and storage. The coated disks were press-fit into a TeflonTM holder so that they were flush with the TeflonTM surface, forming a surface with a total diameter of 4 cm. The disk holder was coupled to a shaft leading to a precision rotator. Rotational speeds ranging from 250 to 1750 rpm were used in the experiments.

The TeflonTM holder was submerged so that the coated surface of the disk faced down in a beaker containing 500 ml of cleaning solution. A cleaning experiment would consist of spinning the disk at a fixed speed while an HPLC pump continuously flowed a sample stream of the bulk cleaning solution through a UV detector and then returned it back to the beaker. Experiments were conducted at 24°C, which is below the cloud point of the surfactants studied. The cleaning solution

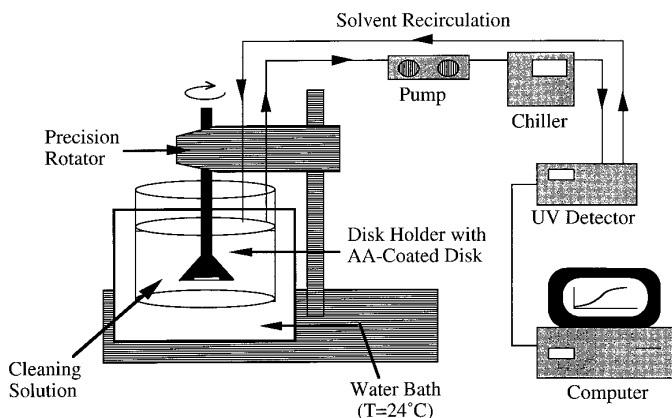


FIG. 3. Experimental setup.

never reached the cloud point as confirmed by the fact that all of the cleaning solutions remained clear during the experiments. A computer was used for data acquisition. The experiments yielded cleaning curves in terms of moles of abietic acid removed as a function of time.

The effect of the surfactant molecular structure on both cleaning rates and film morphology was explored. The following monodisperse polyoxyethylenated nonionic surfactants, provided by Nikkol Chemicals, were used, C_8E_5 , $C_{10}E_5$, $C_{12}E_5$, $C_{12}E_8$, and $C_{16}E_8$. Key properties of these surfactants are summarized in Table 1. The surfactants C_8E_5 and $C_{12}E_8$ were selected because they have similar HLBs, allowing for the influence of surfactant structure on cleaning to be examined with HLB as a fixed variable. The surfactants $C_{10}E_5$ and $C_{12}E_5$ were also selected to allow for the study of a range of alkyl chain lengths from 8 to 12 while the ethoxy chain length is fixed. In order to evaluate the influence of ethoxy chain length on cleaning behavior, $C_{12}E_8$ was compared with $C_{12}E_5$. And $C_{16}E_8$ was selected because its HLB is similar to that of $C_{10}E_5$ and it has the same ethoxy chain length as $C_{12}E_8$. Experimental surfactant concentrations ranged from submicellar conditions to concentrations well above the CMC of all the surfactants employed.

The evolution of the film morphology during the cleaning process was studied by taking photographs of the disk surface. In these experiments, the cleaning process was continuously monitored until it reached a desired point in the cleaning curve. At this time, rotation was stopped, the disk was removed from the apparatus, and the remaining surfactant solution on it was allowed to run off. When dry, the disk was then photographed using a reflective microscope (Reichert MeF2 Metalograph) at $12\times$ magnification.

RESULTS AND DISCUSSION

Cleaning Curves and Cleaning Mechanisms

Figure 5 shows the results of cleaning experiments for a series of surfactants in water at $6.0 \times 10^{-5} M$, which is submicellar for all cases, and a disk rotational speed of 1500 rpm. The results in Fig. 5 show that varying the alkyl or ethylene oxide chains of the surfactants has a significant effect

Table 1
Properties of the Surfactants Employed

Surfactant	CMC at 25°C (M)	Molecular weight (g/mol)	HLB	Cloud point (°C) (18)
C_8E_5	9.2×10^{-3} (18)	350.5	13.54	60
$C_{10}E_5$	8.1×10^{-4} (19)	378.6	12.54	45
$C_{12}E_5$	6.5×10^{-5} (18)	406.6	11.67	31
$C_{12}E_8$	7.1×10^{-5} (20)	538.8	13.71	77
$C_{16}E_8$	1.6×10^{-6} (19)	594.9	12.41	65

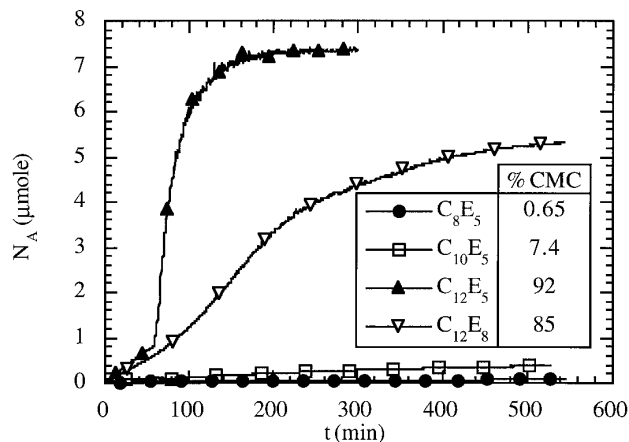


FIG. 5. Cleaning curves of four different surfactants at $6.0 \times 10^{-5} M$ surfactant concentration (symbols are only used to mark curves and do not represent data points), $\omega = 1500$ rpm.

on abietic acid removal. After 9 h, C_8E_5 and $C_{10}E_5$ removed a negligible amount of abietic acid. In fact, at the end of the experiment, the weight of the coated disk had increased slightly instead of decreasing from its preclean weight. This indicated that although some surfactant and water had penetrated into the film, there was not a significant reduction in the film viscosity for mechanical removal. This observation agrees with the studies on lard submersion performed by Cox and Matson (3), in which they observed contaminant weight gain due to surfactant penetration. On the other hand, $C_{12}E_5$ and $C_{12}E_8$ removed the abietic acid from the disks, even though used at concentrations below their CMC. These results indicate that the surfactant has the capability to form micelles containing abietic acid at concentrations lower than their aqueous CMC; in other words, the presence of abietic acid decreases the surfactant CMC. The results in Fig. 5 would seem to indicate that the parameter that controls the effectiveness of the surfactant is its CMC value. For this reason, we examined the cleaning behavior of the different surfactants at concentrations that were fixed percentages of their CMC values.

Figure 6 shows cleaning curves for various surfactants at concentrations equal to 92% of their CMC. The C_xE_5 cleaning processes were all found to exhibit a three-stage cleaning mechanism (this will be discussed below). The second-stage mechanism, for the C_xE_5 series, results in the majority of the contaminant film being removed faster than during the other stages. Therefore, the preferred surfactant in the C_xE_5 series is the one which induces the second stage soonest (C_8E_5). The C_xE_8 surfactants were found to clean by only the solubilization and roll-up mechanisms (this will be shown later). In this case, $C_{16}E_8$ is present at such a low concentration (because of the low value of the CMC) that it cannot remove a large amount of the abietic acid from the disk. The t_c values of the C_xE_5 surfactants are relatively short compared to the time needed by the C_xE_8 surfactants to clean by solubilization and roll-up. Furthermore, second-stage cleaning rates for C_xE_5 surfactants

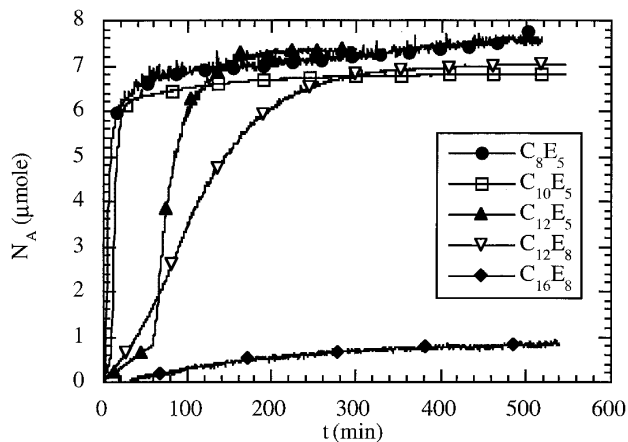


FIG. 6. Cleaning curves of five different surfactants ($\omega = 1500$ rpm) at 92% of their respective CMC. Concentrations used are C_8E_5 at $8.5 \times 10^{-3} M$, $C_{10}E_5$ at $7.5 \times 10^{-4} M$, $C_{12}E_5$ at $6.0 \times 10^{-5} M$, $C_{12}E_8$ at $6.5 \times 10^{-5} M$, and $C_{16}E_8$ at $1.5 \times 10^{-6} M$.

are relatively fast. As a result, the C_xE_8 surfactants tested are less effective under these cleaning conditions.

The trends observed at 92% of the CMC are preserved at concentrations above the CMC. For concentrations that are twice the CMC of the different surfactants (Fig. 7), C_8E_5 is the surfactant that cleans fastest whereas $C_{16}E_8$ is still at a concentration that is too low to remove the film in the time allowed for the experiment.

In Fig. 8 we present cleaning results for the five surfactants at a relatively high concentration ($1.84 \times 10^{-2} M$). C_8E_5 is the best surfactant in terms of time required for total removal. However, at these conditions, $C_{12}E_8$ is able to remove the majority of the contaminant film as fast as $C_{10}E_5$ and faster than $C_{12}E_5$. This is interesting because even though the C_xE_8 surfactants do not exhibit a second stage,

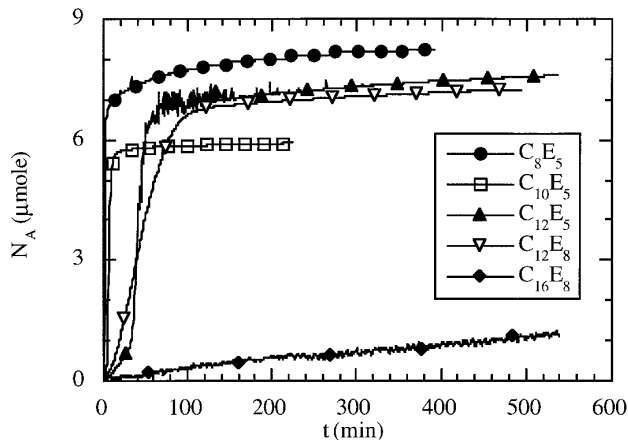


FIG. 7. Cleaning curves of five different surfactants ($\omega = 1500$ rpm) at concentrations twice their respective CMC. Concentrations used are C_8E_5 at $1.8 \times 10^{-2} M$, $C_{10}E_5$ at $1.6 \times 10^{-3} M$, $C_{12}E_5$ at $1.3 \times 10^{-4} M$, $C_{12}E_8$ at $1.4 \times 10^{-4} M$, and $C_{16}E_8$ at $3.2 \times 10^{-6} M$.

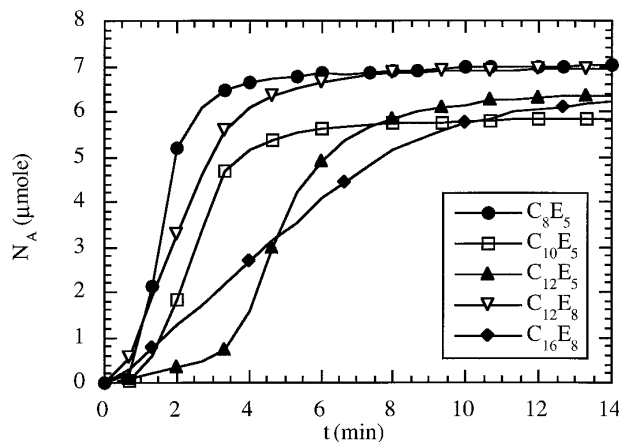
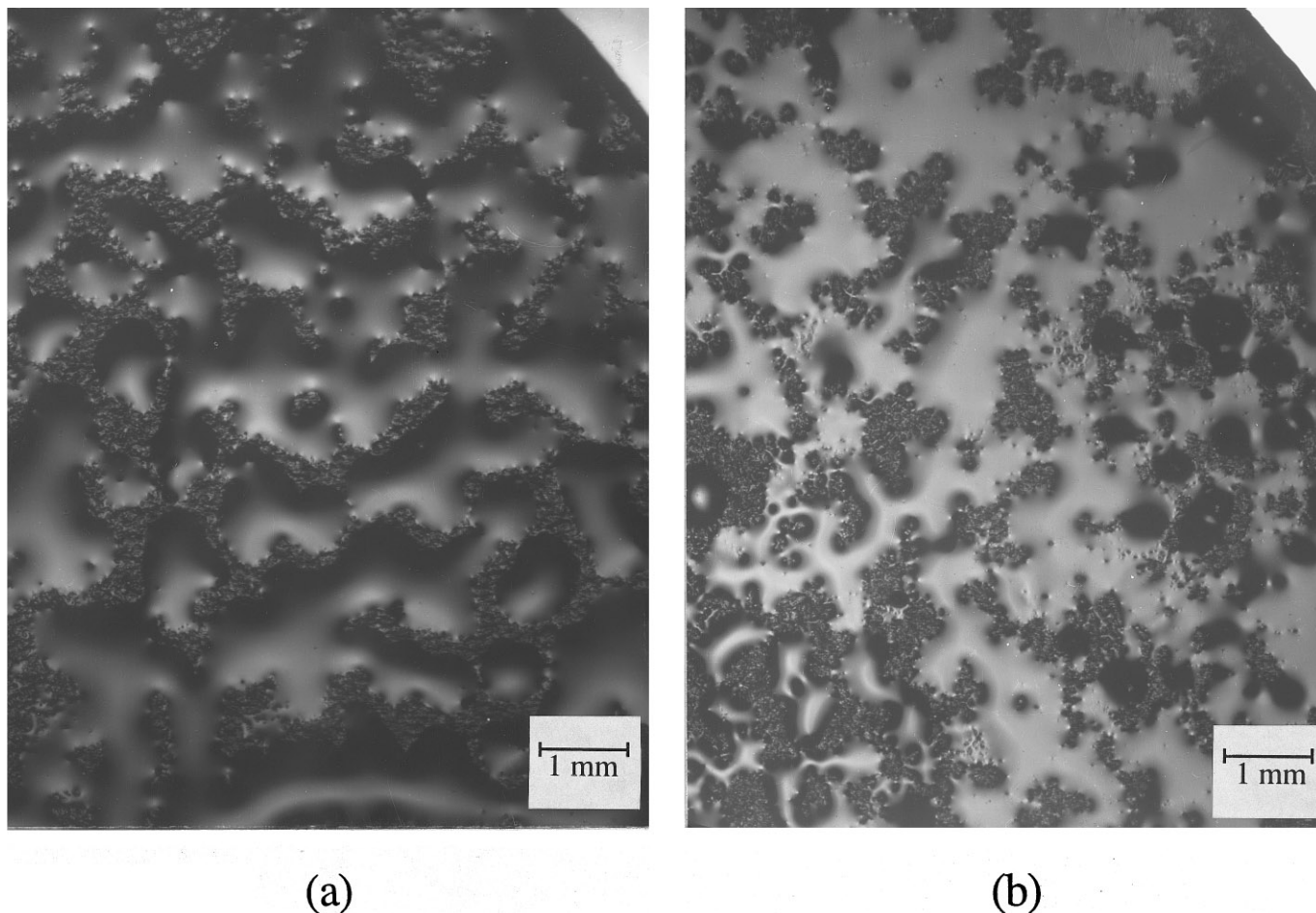


FIG. 8. Cleaning curves of five different surfactants ($\omega = 1500$ rpm) at $1.84 \times 10^{-2} M$ surfactant concentration.

their relatively high solubilization rates are comparable to the rate at which the second stage is completed by the C_xE_5 surfactants. Even $C_{16}E_8$, which did not clean appreciably at 92% and 200% of the CMC yields nearly complete cleaning over the same time scale as $C_{12}E_5$.

Photographic film morphology studies of $C_{12}E_5$ cleaning experiments were performed by Kabin *et al.* (11). These studies have been extended in this work to understand the cleaning behavior of other surfactants. Figure 9a shows a photograph of a disk which was placed in a $1.84 \times 10^{-2} M$ C_8E_5 surfactant solution with no rotation. After 30 min, the abietic acid film appeared to be in the form of liquefied aggregates. However, $C_{12}E_5$ took considerably longer (44 h) to exhibit a similar pattern as shown in Fig. 9b. From this we conclude that in the C_xE_5 surfactant series studied, the shorter alkyl chain favors faster surfactant and water partitioning rates over longer alkyl chain lengths.

In prior work, Kabin *et al.* (11) observed the presence of rivulets during the second stage of cleaning with $C_{12}E_5$. Through these rivulets, the abietic acid flows in a spiral formation from the center of the disk radially outward to the edge of the disk. As aggregates were sheared from the disk surface, they were forced to flow in these rivulets and then were removed from the edge of the disk. Films cleaned with C_8E_5 and $C_{10}E_5$ showed rivulet formation in the second stage, as illustrated in Figure 10a. On the other hand, films cleaned with $C_{12}E_8$ and $C_{16}E_8$ did not exhibit rivulet formation. Figure 10b shows a disk at a point in the cleaning curve with $C_{12}E_8$ at which 40% of the film has been removed (see Fig. 7). Even though this is the part of the cleaning curve where a second stage is observed for C_xE_5 surfactants, no evidence of rivulets is seen for C_xE_8 surfactants. The absence of rivulets was also observed in photographs of $C_{16}E_8$ -cleaned disks over the range of surfactant concentrations and rotational speeds employed in this work. This is because the surfactant did not partition into the film with enough water to lower the contaminant viscosity so as to induce flow. However, solubilization of the contaminant can still occur, which accounts for most of the



(a)

(b)

FIG. 9. Photographs of a disk soaked for: (a) 30 min without rotation in a $1.84 \times 10^{-2} M$ C_8E_5 solution and (b) 44 hours without rotation in a $1.0 \times 10^{-3} M$ $C_{12}E_5$ solution.

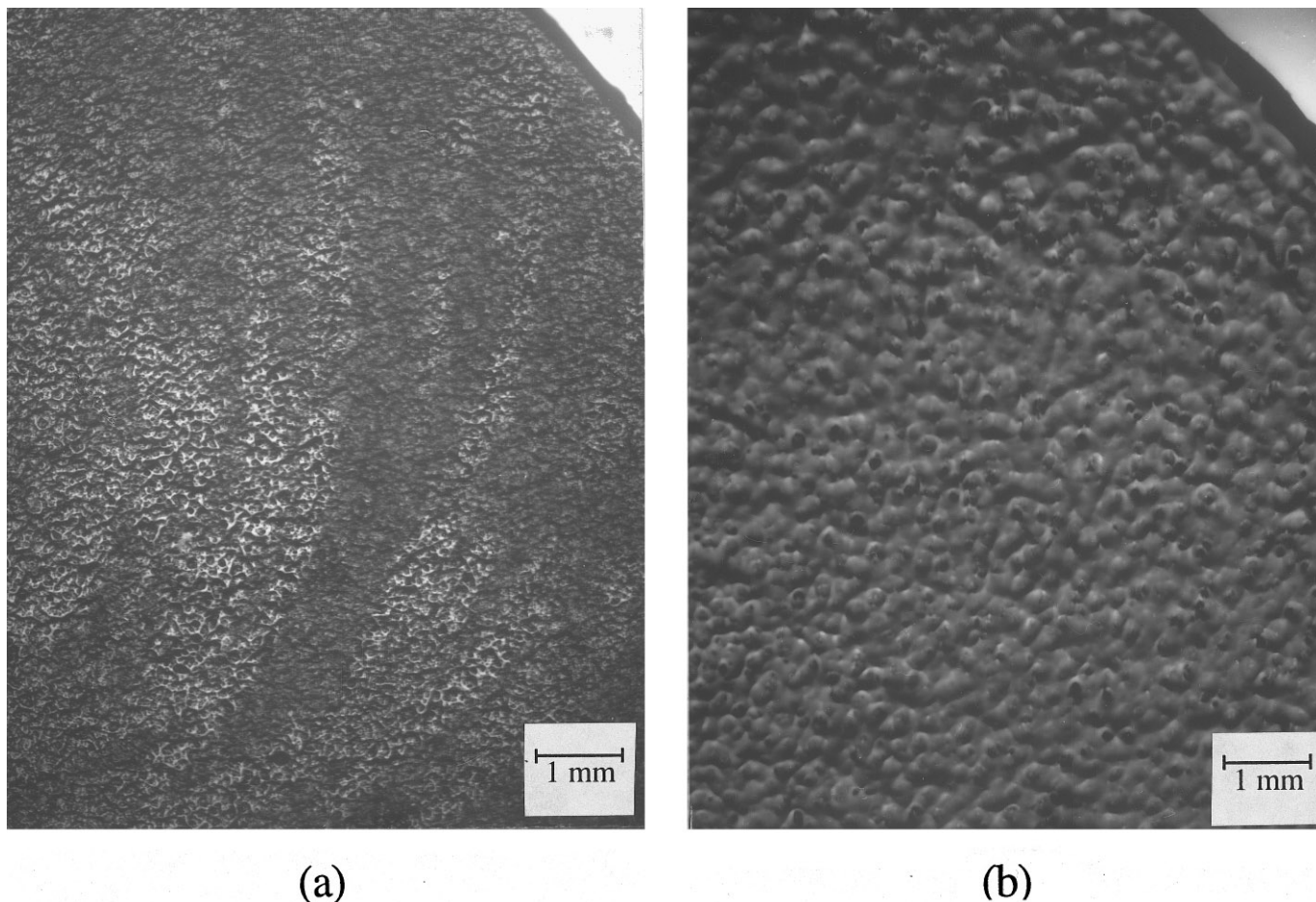
contaminant removal. The C_xE_8 surfactants studied clean by successive solubilization and roll-up mechanisms, and do not exhibit a second stage.

Analysis of Cleaning Rates

The results presented above indicate that the mechanisms through which cleaning occurs depend on the molecular structure of the surfactant. It is interesting, however, to explore how the rates that correspond to each stage in the mechanism are affected by the type of surfactant employed. The first stage of contaminant removal is due to micellar solubilization. Figure 11 shows the first-stage initial rate of contaminant removal for surfactants within a given ethoxy series as a function of HLB. The two points for each surfactant correspond to two separate experiments. The results show that, for a given ethoxy chain length, solubilization rates increase as the alkyl chain length decreases, i.e., as the surfactant becomes more hydrophilic. Figure 11 also indicates that HLB cannot be used as a universal parameter to correlate solubilization rates. Note that C_8E_5 and $C_{12}E_8$ have approximately the same HLB but unexpectedly have quite different first-stage cleaning rates.

The fact that the abietic acid is solubilized faster as the surfactant becomes more hydrophilic leads one to think that there might be interactions between the polar groups of the abietic acid molecules and the ethoxy portion of the surfactant chain in the micellar aggregates.

During the first stage, surfactant partitions into the contaminant film, bringing water along. When the film viscosity is reduced so that it can flow under the influence of the shear stress exerted by the bulk cleaning solution, the second stage begins. This occurs at the transition time, t_c . When sufficient surfactant was used to yield near complete cleaning, t_c was found to decrease with increasing HLB for the C_xE_5 surfactant series (Fig. 12). This trend occurred at each of the surfactant concentrations that resulted in significant contaminant film removal. The decrease of t_c with a decrease in alkyl chain length is a consequence of two different effects: first, smaller alkyl chain surfactants partition more into the film and the fact that they are more hydrophobic indicates that they could solubilize more water into the film (3); second, the surfactants with smaller chains are liquids with lower viscosities so that they are more effective in lowering the viscosity of the film.



(a)

(b)

FIG. 10. Photographs of disks for: (a) 175 rpm in a $1.84 \times 10^{-2} M$ C_8E_5 solution during stage 2, and (b) 1500 rpm in a $1.42 \times 10^{-4} M$ $C_{12}E_8$ solution after 20 min.

The same effects lead to an increase in second-stage rates with HLB, as shown in Fig. 13: a decrease in film viscosity for higher HLBs is reflected in a higher second-stage rate (see Eq. [3]). While Fig. 13 shows cleaning rates at the highest surfactant concentration employed and 92% CMC, the trend of increasing k_2 with increasing HLB was observed at the other surfactant concentrations as well.

Selection of the Optimal Surfactant

In comparing the performance of various surfactants for a specific cleaning application, three important technical aspects should be used to establish which surfactant is best:

- ability of the surfactant to completely remove the contaminant,
- time necessary to perform the cleaning process,
- amount of surfactant employed (i.e., cost).

For the specific problem considered in this work, at sufficient concentrations and rotational speeds, all the surfactants employed can eventually completely remove the film from the surface.

Therefore, economic considerations regarding cleaning time and surfactant cost will prevail in the selection of the best surfactant. We will assume that the cost of the process is directly proportional to cleaning time and amount of surfactant employed. Along these lines, we propose an objective function, defined by

$$\Phi = (M_s)(t^*), \quad [5]$$

which should be proportional to process cost, where M_s is the mass concentration of surfactant in the cleaning solution and t^* is the time required to achieve a certain extent of cleaning. In this study, t^* will be set arbitrarily as the time required to achieve 80% removal of the initial amount of contaminant. The objective function Φ depends on the concentration of surfactant in the cleaning solution and surfactant molecular structure of a given set of experimental conditions. At low surfactant concentrations, t^* becomes very high whereas at high surfactant concentrations t^* becomes ultimately insensitive to concentration. Therefore, the objective function Φ has a minimum, with respect to M_s for a given surfactant. This minimum

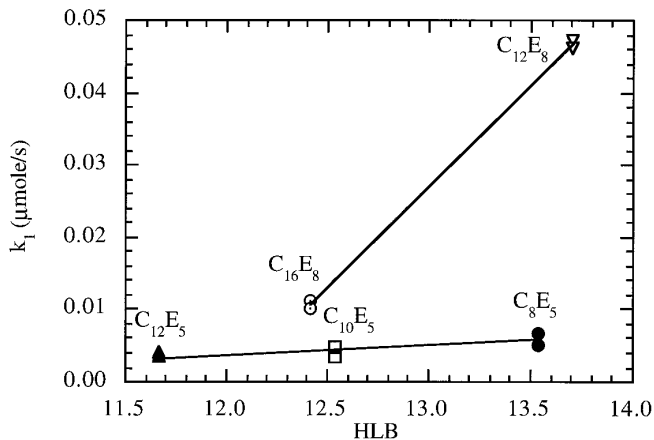


FIG. 11. Initial first-stage cleaning rates for five different surfactants as a function of HLB at $1.84 \times 10^{-2} M$ surfactant concentration and disk rotational speeds of 1500 rpm.

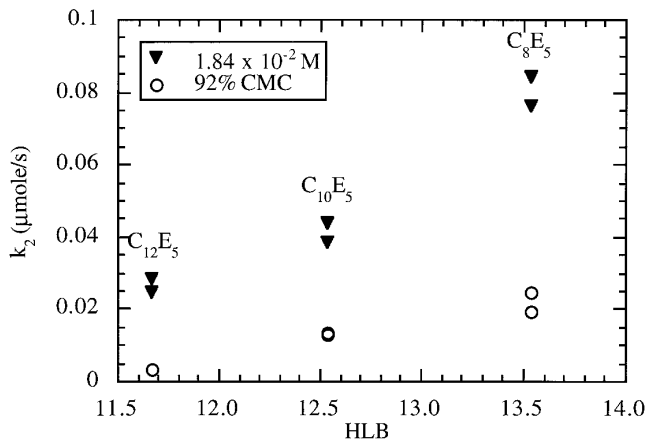


FIG. 13. Second-stage cleaning rates for the three E5 surfactants as a function of HLB at 92% CMC and $1.84 \times 10^{-2} M$ surfactant concentration and disk rotational speeds of 1500 rpm.

determines the optimum concentration of surfactant. On the other hand, if we assume that the cost of surfactant per unit mass is approximately the same within a given family, a comparison of the optima among the different surfactants leads to the selection of the most efficient surfactant to be employed.

The dependence of the objective function on mass concentration of surfactant in the cleaning solution is shown in Fig. 14. Over the range of surfactant concentrations studied, the objective function for each surfactant was found to behave in one of three manners with surfactant concentration, monotonically increasing, decreasing, or exhibiting a minimum. for $C_{12}E_5$ and $C_{16}E_8$ the objective function increased with increasing M_s . Experiments were performed to determine the location of the minimum in the objective function for these surfactants. However, a lower limit was reached in surfactant concentration in which 80% of the contaminant was not removed. This is because the surfactant used in the cleaning solution became saturated with contaminant. Experiments with C_8E_5 produced

an objective function that decreases with increasing M_s . It is believed that at higher surfactant concentrations, the objective function will exhibit a minimum. This, however, could not be experimentally observed because at sufficiently higher surfactant concentrations cleaning occurs too quickly for observation in our experimental apparatus. The objective function for $C_{10}E_5$ and $C_{12}E_8$, however, exhibit minima over the range of surfactant concentrations studied. The minima were observed at 0.61 g/liter ($1.6 \times 10^{-3} M$, twice the CMC) for $C_{10}E_5$ and 0.035 g/liter ($6.5 \times 10^{-5} M$, 92% CMC) for $C_{12}E_8$.

Even though $C_{10}E_5$ and $C_{12}E_8$ exhibit minima over the range of surfactant concentrations studied, they are not the optimal surfactants to use. The minima in the objective function for $C_{10}E_5$ and $C_{12}E_8$ have values of 5.3 and 6.0 g-min/liter, respectively. However, the smallest value of the objective function is 2.4 g-min/liter at 0.024 g/liter ($6.0 \times 10^{-5} M$) obtained with $C_{12}E_5$. This would make $C_{12}E_5$ the optimal surfactant to choose based on the aforementioned criterion. A more realistic

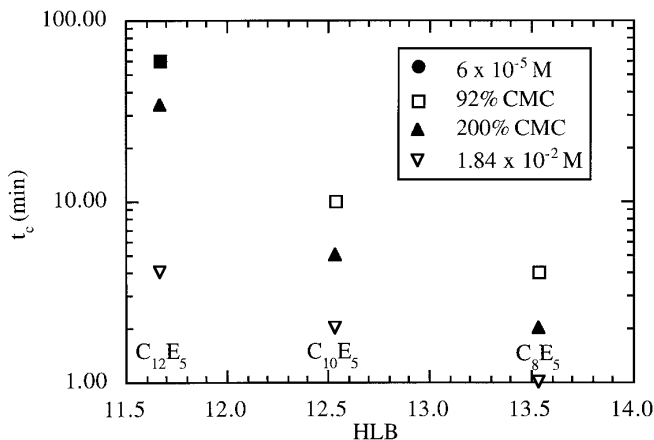


FIG. 12. Stage-two onset time as a function of HLB at disk rotational speeds of 1500 rpm for C_xE_5 surfactants.

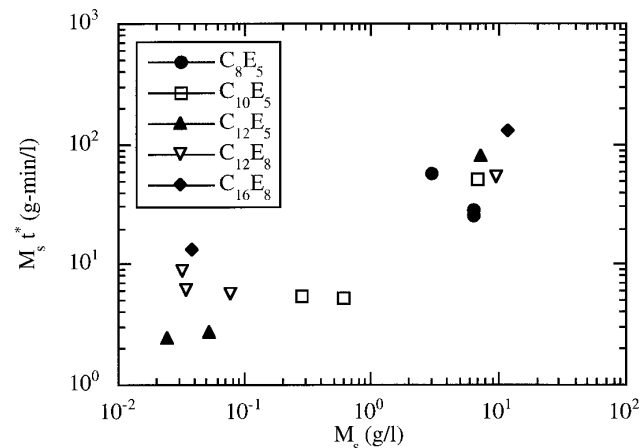


FIG. 14. The objective function for the five surfactants as a function of mass concentration of surfactant in the cleaning solution.

definition of the objective function in an industrial cleaning process would require a knowledge of the economic value of cleaning time, surfactant cost, and other economic factors in implementing a particular cleaning protocol.

CONCLUSIONS

Surfactant structure influences the cleaning mechanisms and cleaning rates associated with abietic acid removal in our experimental system. It was found that the C_xE_5 surfactants studied exhibit a three-stage cleaning mechanism while the C_xE_8 surfactants studied only resulted in the first and third stages of cleaning. As surfactant concentration is increased from submicellar to concentrations in excess of the CMC, the rate of solubilization with C_xE_8 surfactants increases, becoming comparable to the second-stage mechanism observed with C_xE_5 surfactants. From this, we conclude that the conditions at which a surfactant is used are as significant as the choice of a specific surfactant. The optimal surfactant, surfactant concentration, and cleaning time can be chosen on the basis of an objective function analysis such as the one suggested herein.

ACKNOWLEDGMENTS

This work was funded by the Pollution Prevention Research Center at North Carolina State University, the National Science Foundation Program for Environmentally Benign Chemical Synthesis and Processing (Grant No. CTS-9216850), and Corpex Technologies in Research Triangle Park, NC. Northern Telecom Co. in Research Triangle Park, NC, provided the FR-4 laminate. The authors would like to acknowledge the laboratory assistance of Percy McIntyre and the help provided by Inge Simonson on photographic techniques.

REFERENCES

1. Carroll, B., *Colloids Surf. A* **74**, 131 (1993).
2. Miller, C. A., and Raney, K. H., *Colloids Surf. A* **74**, 169 (1993).
3. Cox, M. F., and Matson, T. P., *J. Am. Oil Chem. Soc.* **61**, 1273 (1984).
4. Cox, M. F., *J. Am. Oil Chem. Soc.* **63**, 559 (1986).
5. Cox, M. F., Smith, D. L., and Russell, G. L. *J. Am. Oil Chem. Soc.* **64**, 273 (1987).
6. Rosen, M. J., "Surfactants and Interfacial Phenomena," 2nd ed. Wiley, New York, 1989.
7. Shaeiwitz, J. A., Chan, A. F.-C., Cussler, E. L., and Evans, D. F. *J. Colloid Interface Sci.* **84**, 47 (1981).
8. Ward, A. J. in "Solubilization in Surfactant Aggregates" (S. D. Christian and J. F. Scamehorn, Eds.), p. 237. Dekker, New York, 1995.
9. Beaudoin, S. P., Grant, C. S., and Carbonell, R. G., *Ind. Eng. Chem. Res.* **34**, 3307 (1995).
10. Beaudoin, S. P., Grant, C. S., and Carbonell, R. G., *Ind. Eng. Chem. Res.* **34**, 3318 (1995).
11. Kabin, J. A., Sáez, A. E., Grant, C. S., and Carbonell, R. G., *Ind. Eng. Chem. Res.* **35**, 4494 (1996).
12. Rosen, M. J., *J. Am. Oil Chem. Soc.* **49**, 293 (1972).
13. Rosen, M. J., *J. Am. Oil Chem. Soc.* **51**, 461 (1974).
14. Ueno, M., Takasawa, Y., Miyashige, H., Tabata, Y., and Meguro, K., *Colloid Polym. Sci.* **259**, 751 (1981).
15. Chiu, Y. C., Chen, L. J., and Pien, W. I., *Colloids Surf.* **34**, 23 (1988).
16. Harris, J. C., Anderson, R. M., and Satanek, J., *J. Am. Oil Chem. Soc.* **38**, 123 (1961).
17. Diallo, M. S., Abriola, L. M., and Weber, W. J., Jr., *Env. Sci. and Tech.* **28**, 1829 (1994).
18. Hinze, W. L., and Pramauro, E., *Crit. Rev. Anal. Chem.* **24**, 133 (1993).
19. van Os, N. M., Haak, J. R., and Rupert, L. A. M., "Physico-Chemical Properties of Selected Anionic, Cationic and Nonionic Surfactants." Elsevier, Amsterdam, 1993.
20. Product Specifications Nikkol Chemicals.